Extinction-to-backscatter ratio of Asian dust observed with high-spectral-resolution lidar and Raman lidar

Zhaoyan Liu, Nobuo Sugimoto, and Toshiyuki Murayama

Extinction-to-backscatter ratio or lidar ratio is a key parameter in the issue of backscatter-lidar inversions. The lidar ratio of Asian dust was observed with a high-spectral-resolution lidar and a combined Raman elastic-backscatter lidar during the springs of 1998 and 1999. The measured values range from 42 to 55 sr in most cases, with a mean of 51 sr. These values are significantly larger than those predicted by the Mie computations that incorporate measured Asian dust size distributions and a range of refractive index with a typical value of $1.55-0.005i$. The enhancement of lidar ratio is mostly due to the nonsphericity of dust particles, as indicated by the **T**-matrix calculations for spheroid particles and a number of other theoretical studies. In addition, possible contamination of urban aerosols may also contribute somewhat in optically thin cases. Mie theory, although it can well describe spherical particle scattering, will not be sufficient to represent the scattering characteristics of irregular particles such as Asian dust, especially in directions larger than approximately 90°,when the size parameter is large.

OCIS codes: 010.3640, 010.1110, 010.1310, 290.1310, 290.5850, 280.3640.

1. Introduction

Extinction-to-backscatter ratio or lidar ratio is a key parameter in backscatter-lidar inversions. The lidar ratio is required to retrieve the extinction and backscatter coefficients of aerosols and clouds.[1–3] Methods of lidar-ratio retrieval from backscatter-lidar observation itself as well as extinction and backscatter coefficients have been studied.[4–6] These methods, however, require additional constraints, and as a result their applications are limited to some specific atmospheric conditions. For example, Rayleigh scattering signals from molecules at both sides of target clouds are required in the transmittance method to determine cloud transmittance to constrain the inversion.[5,6] The two-wavelength method requires two-wavelength lidar observations and the similarity of backscatter profiles at two lidar wavelengths as an additional constraint.[4] In practice, lidar observations may cover a large range of different atmospheric conditions, and for most cases the lidar ratio has to be estimated in lidar data analyses. This is especially true for spaceborne lidars that can provide global observations of aerosols and clouds.[7,8] Observational studies are therefore required to establish a climatology of the lidar ratio for an improved lidar-ratio estimation.

A high-spectral-resolution lidar (HSRL)[9] or a combined Raman elastic-backscatter lidar[10] can provide direct observations of the lidar ratio of atmospheric aerosols. An HSRL separates the particulate scattering signal from aerosols or clouds and the Rayleigh scattering signal from atmospheric molecules by means of a narrow-spectral-bandwidth rejection filter. It takes advantage of the fact that molecules have much greater Brownian motion than particles do, and thus backscattered light from molecules is significantly spectrum broadened around the original laser wavelength. Particulate extinction, backscatter coefficients, and consequently particulate lidar ratio can be retrieved with these two scattering signals. A combined Raman elastic-backscatter lidar obtains the same information utilizing molecular Raman scattering.

We developed an HSRL by using an iodine absorption filter and a second-harmonic injection-seeded Nd:YAG laser at the National Institute for Environmental Studies (NIES)[11] and a combined Raman

Z. Liu and N. Sugimoto are with the National Institute for Environmental Studies, 16–2 Onogawa, Tsukuba, Ibaraki, Japan 305-8506. Z. Liu is now with Hampton University, 23 Tyler Street, Hampton, Virginia 23668. T. Murayama is with the Tokyo University of Mercantile Marine, 2–1-6 Etchujima, Koto-ku, Tokyo, Japan 135-8533. N. Sugimoto can be reached at nsugimot@nies.go.jp, and T. Murayama can be reached at murayama@ipc.tosho-u.ac.jp.

Received 28 August 2001; revised manuscript received 9 January 2002.

0003-6935/02/152760-08$15.00/0

elastic-backscatter lidar at the Tokyo University of Mercantile Marine (TUMM).[12] In this paper, we report observations of Asian dust (yellow sand) aerosols with the HSRL at the NIES in Tsukuba (36°05′N, 140°12′E) and the combined Raman elastic-backscatter lidar at TUMM in Tokyo (35°40′N, 139°47′E) during the campaigns of the Asian Dust Observation Network[13] in 1998 and 1999.

Asian dust originating in desert areas of East Asia is a significant phenomenon in the spring season (briefly from March to May). Dust storms often cause aerosol events well beyond the Asian continent; they can even reach the Hawaiian Islands and North America after a long transport over the North Pacific Ocean.[14,15] Because of the large emissions,[16,17] Asian dust may have a significant effect on the atmospheric radiation budget on a global scale. A notable feature of desert dust is nonsphericity, or irregular shape of the particles. An irregular particle has scattering properties that are considerably different from an equivalent sphere, with equal surface or volume and the same refractive index, as demonstrated by a number of laboratory experiments,[18–22] field measurements,[23–25] and semiempirical and rigorous theories.[26–29] Mie theory, which can well describe scattering of a spherical particle, is in general inadequate for the representation of the scattering characteristics of irregular particles, even if the input size distribution and refractive index are correct. This is especially true for backward scattering when the size parameter is larger than approximately 4. The lidar ratio may be enhanced owing to the nonsphericity of dust particles. For example, the lidar ratio calculated by Mishchenko *et al.*[29] for randomly oriented polydisperse spheroids can be 3 times larger than that predicted by the Mie calculation for surface-equivalent spheres with the same size distribution and refractive index.

There are only a few reported measurements of the lidar ratio of dust particles. The instruments used in these studies, e.g., nephelometers and backscattersondes, do not measure backscatter at 180° and single-scattering albedo directly, which are required to determine lidar ratio.[24,25] As a result, the Mie-theory-based model or a semiempirical model that treats irregular particle scattering had to be employed to derive lidar ratios. Recently, a backscsatter nephelometer was improved greatly in capability to detect near-backscatter (178°) and applied to aerosol-lidar ratio measurements combined with an instrument that measures light absorption.[30] Observations with these *in situ* instruments, however, still suffer from the fact that the measurements are performed after the aerosol is dried, and a part of large particles are lost owing to limitations of the inlet system. Hence, direct measurements of aerosol-lidar ratio with a straightforward method such as HSRL and/or Raman lidar are needed to validate these previous observational and theoretical studies and to contribute to an establishment of the required lidar-ratio climatology.

2. Lidar Systems

A. National Institute for Environmental Studies High-Spectral-Resolution Lidar

The NIES HSRL system uses an injection-seeded, pulsed Nd:YAG laser with frequency-doubled output at 532 nm and an iodine vapor absorption cell.[11] This lidar has two detection channels. One channel detects return signals directly, and the other detects return signals through the iodine cell. The cell works as a narrow-spectral-band rejection filter to remove the particulate scattering component from aerosols and clouds in lidar return signals. The laser wavelength is tunable over a range wider than 20 GHz, which covers three iodine absorption lines, 1109, 1110, and 1111. When the laser wavelength is tuned to the center of an absorption line, the spectrally narrow particulate scattering component is absorbed in the iodine cell. On the other hand, the molecular scattering component that has a widely Doppler-broadened spectrum can transmit partially through the iodine cell. Thus only the molecular component is detected in this channel. In the second channel, both the particulate and the molecular components are detected.

From these two channel signals, particulate- and molecular-scattering signals can be determined. The particulate backscatter coefficient is derived simply from the ratio of particulate and molecular signals, with a reference molecular-scattering profile that can be calculated from local temperature and pressure data. The particulate extinction coefficient can be retrieved from the molecular signal, which contains the particulate extinction term as well as molecular-backscattering and extinction terms. A detailed description of the HSRL method is given in our previous paper.[11]

Observations of Asian dust with this HSRL began in 1998. A depolarization measurement function was added in April 1999. A depolarization of the backscattered signals can be caused by the nonsphericity of particles. The total depolarization ratio is defined as the ratio of the perpendicular component to the parallel component of the backscattered signal. The particulate depolarization ratio (PDR) and the molecular depolarization ratio (MDR) refer to the scattering by aerosol particles and by molecules, respectively. PDR is a useful indicator of nonsphericity for the identification of ice clouds[31] and dust layers.[12,32] PDR can be derived from observed total-to-Rayleigh backscatter ratio (BR) and TDR by the following equation:

$$\mathrm{PDR} = \frac{\mathrm{TDR}(\mathrm{BR} + \mathrm{BR} \times \mathrm{MDR} - \mathrm{MDR}) - \mathrm{MDR}}{\mathrm{BR} - 1 + \mathrm{BR} \times \mathrm{MDR} - \mathrm{TDR}}. \quad (1)$$

MDR can be found in the literature,[33] and MDR = 0.014 was used in this work.

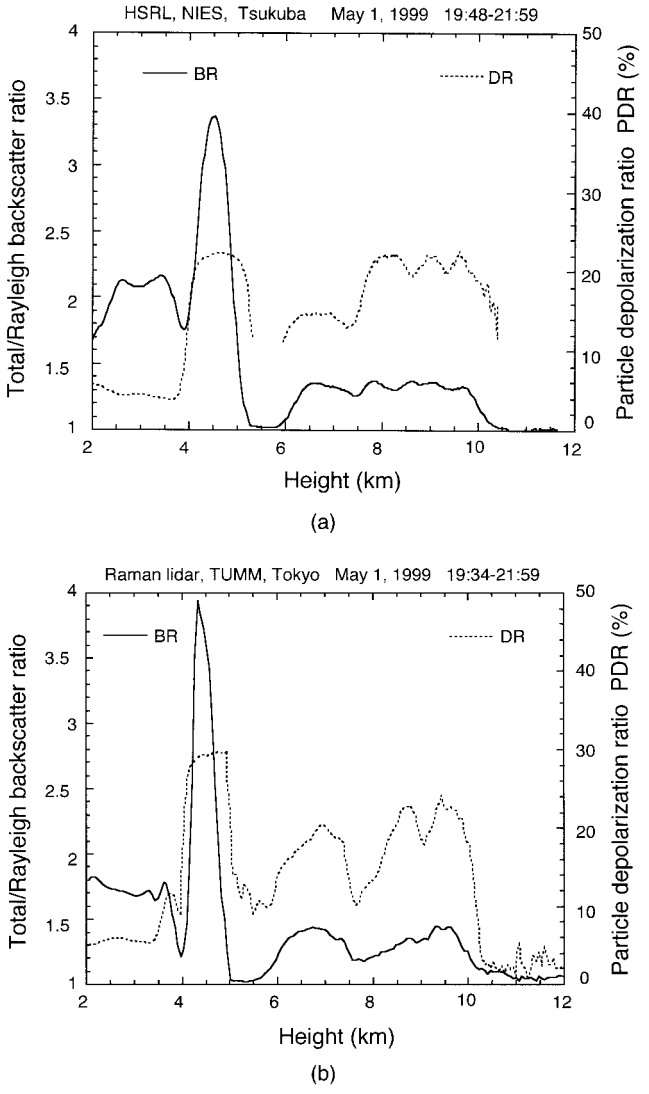

Fig. 1. Example of simultaneously observed BR and PDR at (a) NIES and (b) TUMM on the night of 1 May 1999.

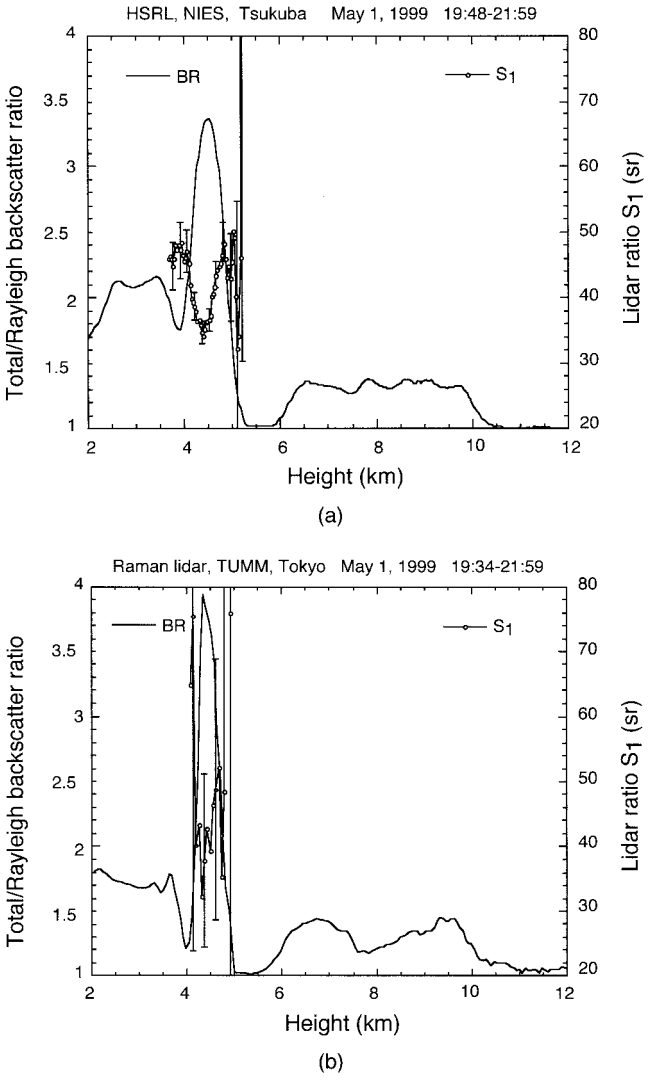

Fig. 2. Retrieved lidar ratios for the lower dust layer shown in Fig. 1, along with BRs for comparison.

B. Tokyo University of Mercantile Marine Lidar

The TUMM lidar is a three-receiver system.[12] Two receivers with different fields of view are used to measure the elastic scattering signals at 532 nm from near field and far field. Both receivers can also provide the observation of aerosol-depolarization ratios. The third is a multipurpose receiver that can be used optionally to detect Raman scattering signals from nitrogen molecules N_2 and/or water vapor molecules H_2O.

With a combined observation of elastic backscattering and N_2 Raman scattering, particulate backscatter and extinction coefficients can be measured independently, and consequently particulate lidar ratio can be determined. The retrieval method is similar to that for HSRL, except that molecular Raman scattering is used instead of molecular Rayleigh scattering. The method was described in detail by Ansmann *et al.*[8] A combined Raman elastic-backscatter lidar is simplistic, compared with an HSRL from a hardware point of view. However, it is more difficult to attain sufficient statistics, because the Raman scattering cross section is much smaller than that of molecular Rayleigh scattering. The correction that is due to the difference between the laser wavelength (532 nm) and Raman-shifted wavelength (607 nm) is made exactly for molecular extinction and approximately for aerosol extinction with an Ångström exponent obtained from Sun-photometer measurements. Errors in derived-extinction coefficients due to the incomplete correction for aerosol scattering are negligibly small compared with the large statistical errors of the Raman lidar signals.

3. Experiment

During the 1998 and 1999 campaigns of the Asian Dust Observation Network, a number of huge dust storms were generated in the deserts of China and Mongolia. In most cases, the dust events were observed with lidars in Japan for several days after the

Table 1. Lidar Ratio Measured with the NIES HSRL

Date	Time	Height (km)	Backscatter Ratio Peak:Mean	Lidar Ratio (sr)
18 March 1998	20:17–21:57	3–10.5	2.6:1.9	73 ± 12[a] (8–10.5 km)
31 March 1998	18:34–20:24	?–6.5	2.4:1.9	43 ± 4[a] (3.5–6.5 km)
19 April 1998	21:51–22:51	?–6.5	5.0:2.3	55 ± 10[b] (2.5–6 km)
20 April 1996	20:45–22:45	1.6–3	2.5:2.1	45 ± 13[b] (2.5–3 km)
1 March 1999	23:07–00:38	3–5	5.2:3.4	49 ± 7.6[b] (3.1–4.5 km)
1 May 1999	19:48–21:54	3.9–5.1 5.9–10.3	3.37:2.57 1.38:1.29	42 ± 4.7[b] (4–5 km)

[a]Height resolution is equal to the analyzed dust layer.
[b]Height resolution is 300 m.

storms. Sky radiometers and optical particle counters also measured greatly increased large-size particles.

Figure 1 shows an example of simultaneously observed BR and PDR at NIES (a) and TUMM (b) on the night of 1 May 1999. A sliding window with a length of 300 m and 420 m, respectively, was used to smooth the HSRL data and combined Raman lidar data to improve signal-to-noise ratio. A similar structure was observed with two lidars. Dust layers at approximately 4–5- and 6–10-km heights can be identified clearly from observed PDRs (dotted curves), where the value of PDR is larger than 10%. An aerosol layer below approximately 4 km can also be seen in observed BRs (solid curves), however, the lower value of DR indicates that this layer mostly consists of spherical particles.

Figure 2 shows retrieved lidar ratios for the lower dust layer in Fig. 1 as well as BRs. Because the retrieval of lidar ratio of optically thin aerosols is very sensitive to noise, we were not able to derive meaningful results for the upper dust layers. The lidar ratio of the lower layer was derived as a function of the height from both lidars. The profiles of lidar ratio are similar. To compare the lidar ratio values at the two sites, we averaged lidar ratios over the height of the dust layer. The height-averaged value is 42 ± 4.7 sr (4–5 km) at NIES and 43 ± 6.3 sr (4.2–4.6 km) at TUMM. The standard deviations reflect both noise and possible variations in true lidar ratio with height. The results from the two measurements agree very well. This kind of comparison is useful for validating the measurement methods and observed results. However, there was only one case that could be used for intercomparison, because the TUMM lidar was not operated frequently to measure lidar ratio during the 1998 and 1999 campaigns but is accumulating similar data for subsequent campaigns.

Lidar ratio was derived with HSRL selectively for heavy dust events. Table 1 lists observation date, time over which lidar profiles were averaged, height of dust layers, peak and mean of total-to-Rayleigh backscatter ratio, and lidar ratio. All of the data in Table 1 were taken at night. The daytime observation was not possible, because we used a photon-counting system. Only the 1 May 1999 case was performed with the polarization measurement. For the other cases, the elevated dust layers were identified from the TUMM lidar-polarization measurement. The height of the lower boundaries of dust layers was not determined clearly in some cases where the depolarization measurement was not conducted, and there were lower local aerosols at the NIES lidar site. The lidar ratio was retrieved with a range resolution of 300 m. The value of the lidar ratio given in Table 1 was averaged within the dust layer. The standard deviation was calculated from derived lidar ratios at different heights within the dust layer. It contains noise and actual change of lidar ratio along the path of laser beam in the layer. For optically thin dust layers with a low signal-to-noise ratio, i.e., 18 March 1998 and 31 March 1998 cases, a larger range resolution equal to the thickness of dust layers was used to improve the retrieval. In this case, the standard deviation reflects mainly the noise effect.

4. Comparisons and Discussions

Lidar ratio of atmospheric aerosols can span, in general, over 1 order of magnitude from approximately 10 to 100 sr. Its value is, as predicted by Mie calculations[34] small for coarse-particle-dominated maritime and desert aerosols and large for fine-particle-dominated continental aerosols. A typical value for desert dust is approximately 20 sr at 532 nm. However, our findings of height-averaged lidar ratio of Asian dusts in this study are mostly within 42–55 sr, with an exceptionally large case of 73 sr as listed in Table 1. These findings are much larger than the predicted typical value, suggesting a significant enhancement in Asian dust lidar ratio.

We also conducted Mie analyses for comparison. Volume size distributions shown in Fig. 3(a) have been used. These size distributions were derived

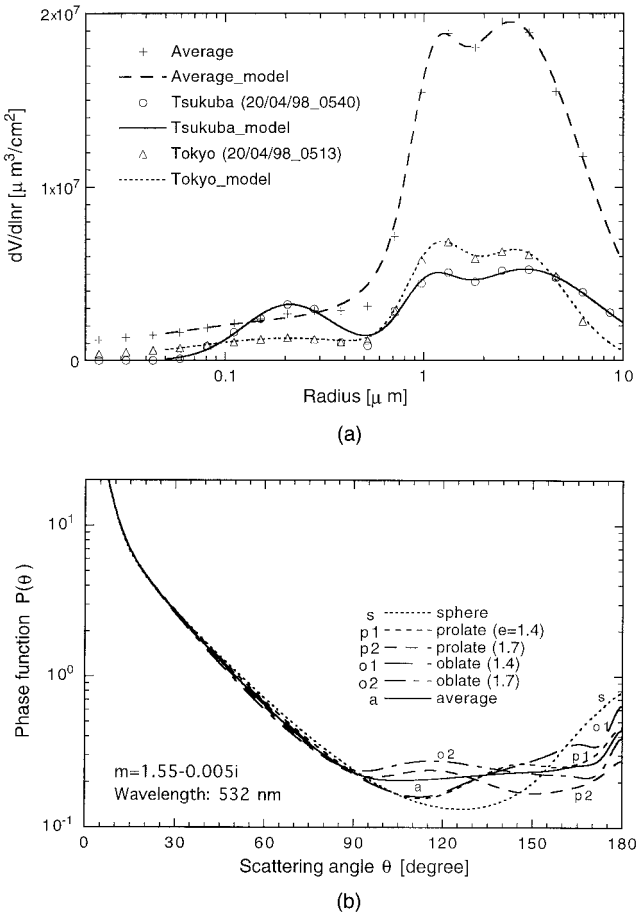

Fig. 3. (a) Average of volume size distributions obtained with sky radiometers at Tokyo, Tsukuba, Okayama, and Sapporo on 19–21 April 1998, along with distributions for Tokyo and Tsukuba and curve-fitted multimode log-normal models of these distributions. (b) Phase functions computed with Mie theory for equivalent spheres and the **T**-matrix code for randomly oriented oblate and prolate spheroids with the average size distribution in (a) and a typical refractive index of $m = 1.55–0.005i$ for two long-to-short dimension ratios of $e = 1.4$ and 1.7. Lower values of phase function at 180 ° for the spheroids than that for the equivalent spheres show the enhancement in lidar ratio of irregular particles [see Eq. (3)].

with sky radiometers in Japan for a heavy Asian dust event that originated near the Gobi desert, was delivered to Japan, and lasted for few days in April 1998.[13] Figure 3(a) presents the average of size distributions measured at the Tsukuba, Tokyo, Okayama, and Sapporo sites on 19–21 April 1998, along with the size distributions at the Tsukuba and Tokyo sites, as well as curve-fitted multimode log-normal models of these distributions. Similar bimodal structures are seen for coarse particles at most sites. The result is consistent with a previous observational study of Asian dusts in Japan.[35] A distinctive fine mode centered near 0.2 μm is seen in the distribution for Tsukuba. Such a remarkable fine mode, however, was not found at other sites, which suggests that this fine mode originates from another local source. Such a mode is characteristic of an urban polluted atmosphere.[36] In practice, the fine-mode particles could be mixed partially in the dust layer in very small amounts. This is supported by our depolarization measurement: The generally high value of measured depolarization ratios within dust layers indicates a low mixing of these fine-mode aerosols. Furthermore, sky radiometers only provide integrated information of the size distribution of total particles from the ground to the top of the atmosphere. From these facts, we can reasonably conclude that a volume size distribution dominated by a coarse mode such as the averaged one in Fig. 3(a) is typical for heavy Asian dust events.

A value of $m = 1.55–0.005i$[24] has been employed as representative for refractive index. In fact, a value of approximately 0.0047 of imaginary part at 532 nm was observed recently on the basis of an absorption measurement of soil particles sampled at Chinese desert area.[37] The same value of the real part of 1.55 along with observed values of the imaginary part in the visible region are used in the modeling of Asian dust aerosols for satellite radiance studies.[37] A slightly different value of $m = 1.53–0.0063i$ has been employed in previous Mie computations for mineral particles.[34] The typical value of refractive index in our calculation is therefore reasonable, though the true value may vary with location and/or dust events.

The computed phase function for volume-equal spherical particles with Mie theory with the averaged size distribution and $m = 1.55–0.005i$ is presented in Fig. 3(b), along with those computed for spheroid particles, which will be described later in this paper. They have been normalized with

$$\frac{1}{2}\int_0^{\pi} \sin(\theta)\, P(\theta)\, \mathrm{d}\theta = 1. \tag{2}$$

Here P is the phase function; θ is the scattering angle. The lidar ratio can be calculated with the following relation:

$$S = \frac{\text{Extinction}}{\text{Backscatter}} = \frac{4\pi}{\omega P(180°)}, \tag{3}$$

where $P(180°)$ is the value of phase function at the scattering angle of 180°. ω is the single-scattering albedo and is given by

$$\omega = \frac{\int_0^{\infty} C_{\text{sca}}(r) n(r)\, \mathrm{d}r}{\int_0^{\infty} C_{\text{ext}}(r) n(r)\, \mathrm{d}r} = 1 - \frac{\int_0^{\infty} C_{\text{abs}}(r) n(r)\, \mathrm{d}r}{\int_0^{\infty} C_{\text{ext}}(r) n(r)\, \mathrm{d}r}. \tag{4}$$

Here $C_{\text{sca}}(r)$, $C_{\text{abs}}(r)$, and $C_{\text{ext}}(r)$ are the nondisperse particle scattering, absorption, and extinction coefficients for a given radius r. They are all obtained from the computations along with phase functions. $n(r)$ is the number size distribution function of particles and can be derived from the volume size distribution, as shown in Fig. 3(a). The calculated lidar

Table 2. Lidar Ratios Computed by Means of Mie Theory and T-Matrix Method[a]

Size distribution	Lidar ratio [sr]						
	Sphere			Spheroid			
	$m_r = 1.55$, $m_i = 0.005$	$m_i = 0.005$, $m_r = 1.50–1.60$	$m_r = 1.55$, $m_i = 0.001–0.010$	Oblate ($e = 1.4$)	Oblate (1.7)	Prolate (1.4)	Prolate (1.7)
				$m = 1.55–0.005i$			
Tokyo	19.3	28.6–13.4	14.5–25.3	23.4	36.9	32.5	51.2
Tsukuba	27.4	38.4–20.0	21.4–34.7	34.0	49.7	41.8	59.3
Average	17.9	27.3–12.1	13.3–23.7	21.7	35.5	30.5	50.7

[a] e, the long-to-short dimention ratio; m: the complex infractive index; m_r: the real part of the complex refractive index; m_i: the imaginary part.

ratio is 17.9 sr for the average size distribution and 19.3 and 27.4 sr for the distribution for Tokyo and Tsukuba, respectively. The relatively large value for Tsukuba is due to the fine mode in the size distribution for Tsukuba. Our computations showed that a higher mixing ratio of the fine mode can cause a larger lidar ratio, with a maximum of 45.5 sr. Hence, a significant contamination by the fine-mode particles can cause large lidar ratios for optically thin dust layers. However, for most measured lidar ratios in this paper, the contributions of fine modes are not significant, because most of the analyzed dust layers in this paper are optically thick.

To see the possible effect of refractive index on lidar-ratio prediction, we conducted Mie calculations with the size distributions in Fig. 3(a) for two cases of changing refractive index. Case 1 is with a fixed imaginary part of 0.005 and a varying real part of 1.50–1.60, whereas case 2 is with a fixed real part of 1.55 and a varying imaginary part of 0.001–0.01. All lidar ratios computed in this paper are listed in Table 2. The lidar ratio for the average size distribution is approximately 12–27 and 13–24 sr, respectively, for case 1 and case 2. It is shown that ether a smaller real part or a larger imaginary part can result in a higher lidar ratio. For a more accurate computation of lidar ratios, exact values of both the real and imaginary parts are required. Nevertheless, comparisons of the observed values with these Mie results still suggest the lidar-ratio enhancement of Asian dust.

This enhancement is mostly due to the irregular shape or the nonsphericity of Asian dust particles, although for some cases the dust layer might be polluted with fine-mode particles, which tend to cause larger lidar ratios. A previous observation of an Asian dust event showed that the particle long-to-short dimension ratio e can be as large as 2.5 (Ref.38). To study the effect of dust particle nonsphericity, we have computed phase functions, as shown in Fig. 3(b), for randomly oriented single-shape spheroids using the **T**-matrix code[39] with the same size distributions and typical refractive index, as in our Mie calculations. Two typical values of $e = 1.4$ and 1.7 were assumed for both oblate and prolate spheroids. As seen in Fig. 3(b), although the spheroid phase functions have a more complex structure in backward directions that are larger than approximately 90°, they all have a smaller value at 180° than that for the equivalent spheres. This suppression in backscattering that is due to the nonsphericity causes the enhancement in lidar ratios. Our computations showed that the nonsphericity does not cause significant difference in the single-scattering albedo from equivalent spheres. Values of the resulting lidar ratio are also given in Table 2. They can be as large as approximately 3 times those for the equivalent spheres.

Note, however, that the lidar ratio also depends on the particle shape distribution. In fact, the particle shape of Asian dust particles is very complex, with a broad distribution of e.[38] As a result, the real phase function of Asian dust may differ greatly from that predicted for single-shape particles. We can demonstrate this difference simply by averaging these phase functions for oblate and prolate particles. The averaged phase function is also presented in Fig. 3(b). It has a structure simpler than that of single-shape phase functions. Nevertheless, such a study with **T**-matrix is very useful in understanding the role of the nonsphericity in dust particle scattering.

It should also be noted that, beside particle nonsphericity, particle size and refractive index also play an important role in the particle scattering as discussed above. Liu *et al.*[40] demonstrated that particle size, refractive index, and particle shape can produce a similar optical effect. Nakajima *et al.*[24] have also shown that effects on the light scattering of irregular particles and absorbing spheres can be similar. Large lidar ratios of continental aerosols due to the small sizes[30] or high absorption[41] have been reported. In fact, the exceptionally high value of 73 sr measured on 18 March 1998 in this study is likely due to a combined effect of the dust particle nonsphericity and the contamination of fine-mode particles and/or some high-absorption particles. In this case, the dust layer is optically thin, and therefore the contribution of fine-mode particles may be significant. In addition, the size of dust particles ascending to the high troposphere (8–10.5 km) may be itself relatively small and consequently cause larger lidar ratio. All of these observation studies support the theoretical predictions quite well.

The published studies of the measurements of lidar ratio of desert dust are few. Nakajima *et al.*[24] re-

ported measurements of Asian dust events with a polar nephelometer at Nagasaki. Although the polar nephelometer could not provide direct measurements of phase functions at 180° and single-scattering albedo, which are required for determining lidar ratio [refer to Eq. (3)], with the aid of the semiempirical theory for irregular particles by Pollack and Cuzzi [26] they derived lidar ratios of Asian dusts. Their values range from 49 to 87 sr at 500 nm, which is much larger than their computed value for the volume-equivalent spheres. They pointed out that the suppression of backscattering induced by the particle nonsphericity is the reason for lidar-ratio enhancement. They also demonstrated that, measured phase functions of dust particles can be fitted by either the semiempirical theory or Mie theory with a large fictitious value of refractive index, showing some similarity between the light scattering by irregular particles and the absorbing particles.

Rosen *et al.*[25] reported a measurement method of lidar ratio using a nephelometer and a backscattersonde. They measured lidar-ratio values of 41.6 sr at 490 nm and 32.2 sr at 700 nm with one standard deviation of 20% for near-surface particles after a modest dust storm in New Mexico. The researchers reported, however, that no apparent lidar-ratio enhancement was found when compared with their Mie computation results. This may be due partially to the smaller particle sizes. The large-mode geometric mean radius of the size distributions associated with their measurements is approximately 0.3 μm, yielding a size parameter smaller than 5, which is the critical value for distinctive nonspherical effects. Waggoner *et al.*[42] carried out measurements of aerosols at a 15-m height in urban Seattle using a more direct method with a lidar and a nephelometer. They derived a high scatter-to-backscatter ratio of 84 ± 11 sr. The value of lidar ratio is possibly larger than 84 sr if aerosol absorption is considered. Waggoner *et al.* also indicated the large observed value is probably due to the irregular shape of aerosol particles.

Both theories and measurements have indicated that Mie theory is inadequate to describe light scattering of irregular particles when the size parameter is large. The measurement of Asian dust with the HSRL and combined Raman lidar in this paper provides evidence of the lidar-ratio enhancement of Asian dust particles owing to the nonsphericity of irregular particles.

5. Conclusions

An observation study of lidar ratio of Asian dust events in 1998 and 1999 with an HSRL in Tsukuba and a combined Raman elastic-backscatter lidar in Tokyo has been reported in this paper. The measured height-averaged values of lidar ratio ranged mostly from 42 to 55 sr, with a relatively large case of 73 sr. These values have a mean of 51 sr.

Comparisons with the Mie computed values of lidar ratio for volume-equivalent spherical particles indicated that observed values are significantly enhanced. This enhancement is caused mostly by the nonsphericity of dust particles. A computation study with the **T**-matrix method for the angular scattering of randomly oriented oblate and prolate spheroids also suggested an enhancement in the lidar ratio of irregular particles, as predicted by a large number of other theoretical studies. It was revealed that Mie theory is inadequate to describe the light scattering of irregular particles such as Asian dust in backward directions.

The present study provided a direct measurement of the lidar ratio of Asian dust with lidars that is useful in the validation of previous theoretical and experimental studies. Such a study is also needed to establish the climatology of aerosol-lidar ratios. Because of the complexity of the size and shape distribution of dust particles, further observations of lidar ratio of dust aerosols are required.

The combined Raman elastic-backscatter lidar research at TUMM was supported by Core Research for Evolutional Science and Technology of Japan Science and Technology. We gratefully acknowledge Michael Mishchenko and Peter Voelger for their valuable help with the **T**-matrix calculation, Hajime Fukushima for the useful discussion on modeling Asian dust aerosols, and Ali Omar for his comments and help during the preparation of the manuscript. The reviewers' invaluable comments are also greatly acknowledged.

References

1. F. G. Fernald, B. M. Herman, and J. A. Reagan, "Determination of aerosol height distributions by lidar," J. Appl. Meteorol. **11,** 482–489 (1972).
2. J. D. Klett, "Lidar inversion with variable backscatter/extinction ratios," Appl. Opt. **24,** 1638–1643 (1985).
3. Y. Sasano and H. Nakane, "Significance of the extinction/backscatter ratio and the boundary value term in the solution for the two-component lidar equation," Appl. Opt. **23,** 11–12 (1984).
4. Y. Sasano and E. V. Browell, "Light scattering characteristics of various aerosol types derived from multiple wavelength lidar observations," Appl. Opt. **28,** 1670–1679 (1989).
5. K. Sassen and B. S. Cho, "Subvisual-thin cirrus lidar dataset for satellite verification and climatological research," J. Appl. Meteorol. **31,** 1275–1285 (1992).
6. S. A. Young, "Analysis of lidar backscatter profiles in optical thin clouds," Appl. Opt. **30,** 7019–7031 (1995).
7. D. Winker, "Global observations of aerosols and clouds from combined lidar and passive instruments to improve radiation budget and climate studies," Earth Obs. **11,** 22–25 (1999).
8. Z. Liu, P. Voelger, and N. Sugimoto, "Simulations of the observation of clouds and aerosols with the Experimental Lidar in Space Equipment system," Appl. Opt. **39,** 3120–3137 (2000).
9. S. T. Shipley, D. H. Tracy, E. W. Eloranta, J. T. Trauger, J. T. Sroga, F. L. Roesler, and J. A. Weinman, "High spectral resolution lidar to measure optical scattering properties of atmospheric aerosols. 1. Theory and instrumentation," Appl. Opt. **22,** 3716–3724 (1983).
10. A. Ansmann, M. Riebessell, U. Wandinger, C. Weitkamp, E. Voss, W. Lahmann, and W. Michealis, "Combined Raman elastic-backscatter lidar for vertical profiling of moisture, aerosol extinction, backscatter, and lidar ratio," Appl. Phys. B **55,** 18–28, 1992.

11. Z. Liu, I. Matsui, and N. Sugimoto, "High-spectral-resolution lidar using an iodine absorption filter for atmospheric measurements," Opt. Eng. **38,** 1661–1670 (1999).
12. T. Murayama, H. Okamoto, N. Kaneyasu, H. Kamataki, and K. Miura, "Application of lidar depolarization measurement in the atmospheric boundary layer: effects of dust and sea-salt particles," J. Geophys. Res. **104,** 31,781–31,792 (1999).
13. T. Murayama, N. Sugimoto, I. Uno, K. Kinoshita, K. Aoki, N. Hagiwara, Z. Liu, I. Matsui, T. Sakai, T. Shibata, K. Arao, B.-J. Sohn, J.-G. Won, S.-C. Yoon, T. Li, J. Zhou, H. Hu, M. Abo, K. Iokibe, R. Koga, and Y. Iwasaka, "Ground-based network observation of Asian dust events of April 1998 in East Asia," J. Geophys. Res. **106,** 18,345–18,359 (2001).
14. G. E. Shaw, "Transport of Asian desert aerosol to the Hawaiian Islands," J. Appl. Meteorol. **19,** 1254–1259 (1980).
15. J. R. Parrington, W. H. Zoller, and N. K. Aras, "Asian dust: seasonal transport to the Hawaiian Islands," Science **220,** 195–197 (1983).
16. M. Uematsu, R. A. Duce, J. M. Prospero, L. Chen, J. T. Merrill, and R. L. McDonald, "Transport of mineral aerosol from Asia over the North Pacific Ocean," J. Geophys. Res. **88,** 5343–5352 (1983).
17. Y. Iwasaka, H. Minoura, and K. Nagaya, "The transport and spatial scale of Asian dust-storm clouds: a case study of the dust-storm event of April 1979," Tellus B **35,** 189–196 (1983).
18. A. C. Holland and G. Gagne, "The scattering of polarized light by polydisperse systems of irregular particles," Appl. Opt. **9,** 1113–1121 (1970).
19. R. H. Zerull, R. H. Giese, and K. Weiss, "Scattering functions of nonspherical dielectric and absorbing particles vs. Mie theory," Appl. Opt. **16,** 777–778 (1977).
20. R. J. Perry, A. J. Hunt, and D. R. Huffman, "Experimental determinations of Mueller scattering matrices for nonspherical particles," Appl. Opt. **17,** 2700–2710 (1978).
21. R. G. Pinnick, D. E. Carroll, and D. J. Hofmann, "Polarized light scattered from monodisperse randomly oriented nonspherical aerosols: measurements," Appl. Opt. **15,** 384–393 (1976).
22. S. C. Hill, C. Hill, and P. W. Barber, "Light scattering by size/shape distribution of soil particles and spheroids," Appl. Opt. **23,** 1025–1031 (1984).
23. G. W. Grams, I. H. Blifford, Jr., D. A. Gillette, and P. B. Russell, "Complex index of refraction of air borne soil particles," J. Appl. Meteor. **13,** 459–471 (1974).
24. T. Nakajima, M. Tanaka, M. Yamamoto, M. Shiobara, K. Arao, and Y. Nakanishi, "Aerosol optical characteristics in the Yellow Sand events observed in May, 1982 at Nagasaki-Pat II models," J. Meteorol. Soc. Jpn. **67,** 279–291 (1989).
25. J. M. Rosen, R. G. Pinnick, and D. M. Garvey, "Measurement of extinction-to-backscatter ratio for near-surface aerosols," J. Geophys. Res. **102,** 6017–6024 (1997).
26. J. B. Pollack and J. N. Cuzzi, "Scattering by nonspherical particles of size comparable to a wavelength: a new semi-empirical theory and its application to tropospheric aerosols," J. Atmos. Sci. **37,** 861–881 (1980).
27. S. Asano and M. Sato, "Light scattering by randomly oriented spheroidal particles," Appl. Opt. **19,** 962–974 (1980).
28. A. Mugnai and W. J. Wiscombe, "Scattering from nonspherical Chebyshev particles. 3. Variability in angular scattering patterns," Appl. Opt. **28,** 3061–3073 (1989).
29. M. I. Mishchenko, L. D. Travis, R. A. Kahn, and R. A. West, "Modeling phase function for dustlike tropospheric aerosols using a shape mixture of randomly oriented polydisperse spheroids," J. Geophys. Res. **102,** 16,831–16,847 (1997).
30. S. J. Doherty, T. L. Anderson, and R. J. Charlson, "Measurement of the lidar raio for atmospheric aerosols with a 180 ° backscatter nephelometer," Appl. Opt. **38,** 1823–1832 (1999).
31. K. Sassen, "The polarization lidar technique for cloud research: a review and current assessment," Bull. Am. Meteorol. Soc. **72,** 1848–1866 (1991).
32. A. Kobayashi, S. Hayashida, K. Okada, and Y. Iwasaka, "Measurements of the polarization properties of KOSA (Asian dust storm) particles by a laser radar in spring 1983," J. Meteorol. Soc. Jpn. **63,** 144–149 (1985).
33. A. Weber, S. P. S. Porto, L. E. Cheesman, and J. J. Barrett, "High-resolution Raman spectroscopy of gases with cw-laser excitation," J. Opt. Soc. Am. **57,** 9–28 (1967).
34. J. Ackermann, "The extinction-to-backscatter ratio of tropospheric aerosols: a numerical study," J. Atmos. Oceanic Technol. **15,** 1043–1050 (1998).
35. K. Arao, and Y. Ishizaka, "Volume and mass of yellow sand dust in the air over Japan as estimated from atmospheric turbidity," J. Meteorol. Soc. Jpn. **64,** 79–94 (1986).
36. T. Takamura, Y. Sasano, and T. Hayasaka, "Tropospheric aerosol optical properties derived from lidar, sun photometer, and optical particle counter measurements," Appl. Opt. **33,** 7132–7140 (1994).
37. H. Fukushima, M. Toratani, H. Kobayashi, W. Takahashi, A. Tanaka, and B.-J. Sohn, "Atmospheric correction algorithm for satellite ocean color data over the Asian waters," in *Advances in X-Ray Optics*, A. K. Freund, T. Ishikawa, A. M. Khounsary, D. C. Mancini, A. G. Michette, and S. Oestreich, eds., Proc. SPIE **4145,** 18–30 (2000).
38. K. Okada, A. Kobayashi, Y. Iwasaka, H. Naruse, T. Tanaka, and O. Nemoto, "Features of individual Asian dust-storm paticles collected at Nagoya, Japan," J. Meteorol. Soc. Jpn. **65,** 515–521 (1987).
39. M. I. Mishchenko and L. D. Travis, "Capabilities and limitations of a current FORTRAN implementation of the T-matrix method for randomly oriented, rotationally symmetric scatterers," J. Quant. Spectrosc. Radiat. Transfer **60,** 309–324 (1998).
40. Y. Liu, W. P. Arnott, and J. Hallett, "Particle size distribution retrieval from multispectral optical depth: influences of particle nonsphericity and refractive index," J. Geophys. Res. **104,** 31,753–31,762 (1999).
41. A. Ansmann, D. Althausen, U. Wandinger, K. Franke, D. Muller, F. Wagner, and J. Heintzenberg, "Vertical profiling of the Indian aerosol plume with six-wavelength lidar during INDOEX: a first case study," Geophys. Res. Lett. **27,** 963–966 (2000).
42. A. P. Waggoner, N. C. Ahlquist, and R. J. Charlson, "Measurement of the aerosol total scatter-backscatter, " Appl. Opt. **11,** 2886–2889 (1972).